Chemical Papers (2025) 79:3613–3632
https://doi.org/10.1007/s11696-025-04019-2

ORIGINAL PAPER

Competitive adsorption studies for removal of phenolic pollutants using *Cassia fistula*-derived activated carbon

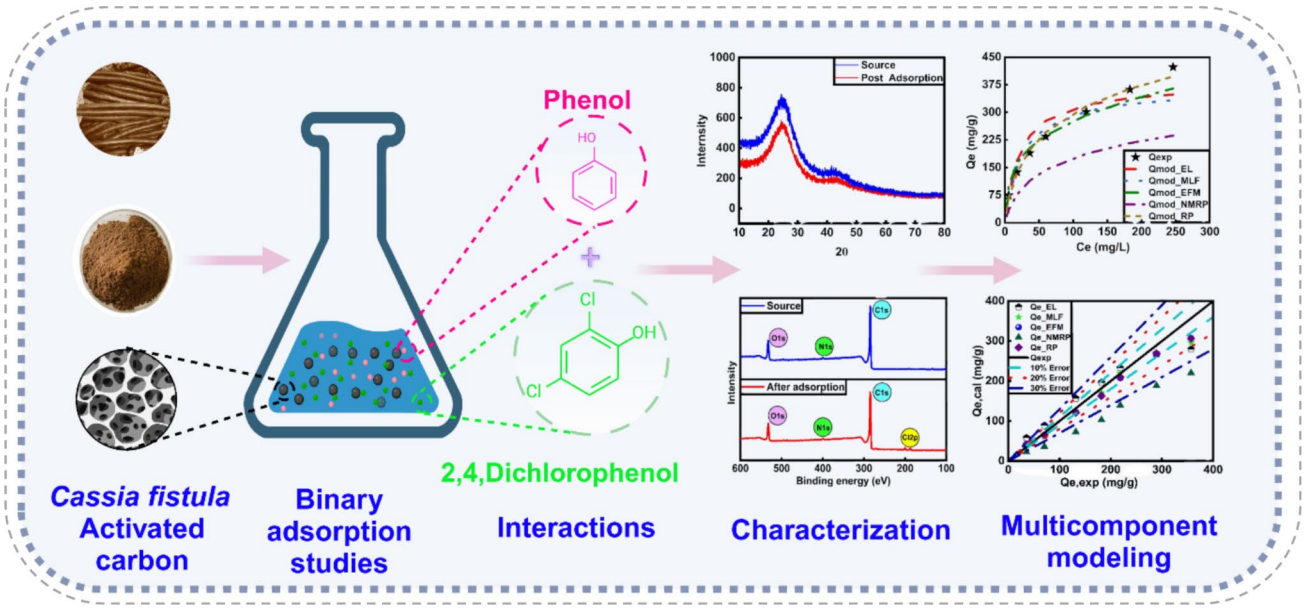
Praveengouda Patil[1] · **Gautham Jeppu**[1] · **Swathi Nayak**[1] · **Chikmagalur Raju Girish**[1]

Received: 18 November 2024 / Accepted: 15 March 2025 / Published online: 16 April 2025
© The Author(s) 2025

Abstract

Industrial effluent is a complex aqueous matrix comprising hazardous substances like phenols and toxic organics, often mixed with nutrients, suspended solids and multiple pollutants. Its constituents vary with industry, making it a significant environmental challenge requiring targeted treatment solutions. So, in the present research, competitive adsorption of phenol and 2,4-Dichlorophenol (2,4-DCP) onto *Cassia fistula*-derived activated carbon (CFPAC) was investigated. In case of phenol adsorption, the modified Langmuir isotherm was found to appropriately align with experimental data and achieving R^2 greater than 0.95 and least Marquardt's percent standard deviation (MPSD), although certain overestimation was observed in the predicted values. Similarly, in case of 2,4-DCP, the experimental values closely aligned with both modified Langmuir and modified Redlich–Peterson isotherm as reflected by higher R^2; however, the estimated values were underestimated. For both pollutants, the adsorption ratio (Rq_i) was less than one. Further, the P-factor (P_{fi}) was exceeding 1 along with positive ΔIE_i implies an antagonistic type of interaction between phenol and 2,4-DCP. The binary desorption of pollutant was effective across for four adsorption–desorption cycles demonstrating the consistent performance of CFPAC.

Graphical Abstract



Keywords *Cassia fistula* · Competitive modelling · Interaction factors · Phenol · Simultaneous adsorption

Extended author information available on the last page of the article

Introduction

India's agricultural sector plays a decisive role in the country's economy, employing a considerable portion of the population and contributing substantially to the GDP. However, the sector encounters numerous challenges, with use of pesticides being a noteworthy factor that carries both positive and negative consequences. A positive aspect would be high crop yield with improved crop quality, which would benefit the farmer's economy. However, the negative aspects could impact the environment by polluting air, soil and water. Additionally, it could also cause health problems in human beings, especially the farmers. The estimated consumption of pesticides for the year 2023–24 was around 2,13,000 metric tons (MT), and the expected demand for the year 2030 is supposed to be 3,43,419 metric tons (Chakraborty et al. 2023). In India, approximately 40% of the total cultivated area undergoes treatment with pesticides, and around 65–70% of this area is subjected to irrigation (Koli and Bhardwaj 2018).

During monsoon, there are high chances that the run-off could carry a portion of the phenolic pesticides and reach any water body, say river water or underground water. Thus, it necessitates management of pesticides in the polluted environments. Phenol and its derivatives, such as 2,4-Dichlorophenol (2,4-DCP), are among the active ingredients present in the pesticides used in the agricultural sector (Shaarani and Hameed 2010). These pollutants are identified as priority pollutants (by USEPA) due to their intrinsic toxic behaviour and resistance towards degradation (K. Zhang et al. 2020). The treatment of these pollutants in mono-mode adsorption has garnered significant attention, as evidenced from the literature (G. Zhang et al. 2024; Melo et al. 2024; Al Rawi et al. 2023).

We are aware of a variety of entities in industrial effluents that can interfere with the adsorption process, necessitating significant attention to their abatement. Many studies, as reported in the literature, have investigated the adsorption of phenol with various ranges of pollutants (Wu et al. 2022; Dong et al. 2021; Tichapondwa, Tshemese, and Mhike 2018; Villar da Gama et al. 2018). While phenol exhibited synergistic interaction when coexisted with resorcinol, cyanide, 2,4-DCP, methyl orange, catechol, aniline, nickel, chromium, lead and cadmium. In contrast, antagonistic behaviour of phenol was also noticed in the presence of cyanide, methylene blue, 2,4-DCP, chromium, cadmium, nitrophenol, nickel and hydroquinone. Further, in few cases non-interaction of phenolic pollutants were also reported during the competitive removal of phenol with resorcinol and mercury (Patil et al. 2023).

These studies comprise of treatment of phenolic pollutants from synthetic wastewater, basically focussing on pulp and paper, the paint industry, textiles and brewery wastewater using activated carbon, biochar, etc. (Körbahti et al. 2007; Mandal, Bar, and Das 2020). Further, they also depict that there is a dearth of studies involving the adsorption of phenol and 2,4-DCP. Thus, there is a need for binary/multicomponent adsorption studies, which can provide information on the affinity of pollutants/adsorbents, inhibition and sidelong interactions between pollutants in binary mixtures and adsorbents.

Each adsorbent has distinct properties for abating pollutants from aqueous media and is popular for offering selective adsorption capabilities for different industrial and environmental applications. Activated carbon is widely used due to its high surface area and porosity, making it effective for organic pollutants. The surface morphology, characterization details and investigation of *Cassia fistula*-derived carbon (CFPAC) to remediate the mono-component phenolic pollutants reported previously (Patil et al. 2024). So, in the present investigation it is emphasized: (a) to characterize the CFPAC used for binary investigation, (b) to perform and analyse binary adsorption of phenol and 2,4-DCP in batch mode, (c) to investigate the regeneration of CFPAC and (d) modelling of the binary adsorption data using different multicomponent isotherm models.

Methodology

Chemicals and methods

Preparation of adsorbent, chemicals used and batch studies

The detailed procedure of *Cassia fistula* pod derived activated carbon (CFPAC) has been discussed elsewhere (Patil et al. 2024). Phenol (C_6H_5OH), 2,4-Dichlorophenol ($C_6H_4Cl_2O$) and hydrochloric acid (HCl) of analytical grade were procured from Merck, India, and were used as adsorbate in the present investigation. A stock solution of 1000 mg/L was prepared by adding 1 g (Phenol/2,4-DCP) in distilled water. Further, equilibrium batch isotherm studies of a binary mixture are carried out to evaluate the impact of one pollutant on other. In isotherm study, the concentration range chosen for first pollutant was 25 to 500 mg/L with dosage of 1.6 g/L, pH 2.0, temperature 20° C and contact time 180 min. To the above setup, each flask was also added with 10 mg/L of the second pollutant. Similar experiments were also conducted for 20 mg/L, 30 mg/L and 40 mg/L of the second pollutant. Further, for the isotherm investigations of second pollutant range remained same as above. The operating conditions were as follows dosage: 0.6 g/L, pH 2.0, temperature 20° C and contact time 120 min. The percentage removal (*%Removal*) and adsorption capability (q_{exp}) were evaluated using the equations (1) and (2).

$$\%Removal = \left(\frac{C_o - C_e}{C_e}\right)100 \quad (1)$$

$$q_{exp.} = \left(\frac{C_o - C_e}{m}\right)V \quad (2)$$

In the above equations, C_o is initial concentration of phenol/2,4-DCP at equilibrium (mg/L), C_e is final concentration of pollutant at equilibrium (mg/L).V is working volume of pollutant under consideration (mL), m is mass of CFPAC (g).

Regeneration and reusability of exhausted CFPAC

Desorption is executed for pollutant, and regeneration is for material. Once the adsorbent is saturated at equilibrium, the regeneration phase is set up. The different types of eluents that could be used for regeneration are dilute hydrochloric acid, sodium hydroxide and Ethylenediaminetetraacetic acid. Further, in some investigations distilled water, ethanol and acetone were also made use (Zhou et al. 2020; Suresh et al. 2021; K. Zhang et al. 2020). In the present investigation, 0.1 N NaOH was employed as eluent wherein, the spent CFPAC was equally transferred to flasks containing 50 mL eluent and experiment was run at 150 rpm, for 180 min at room temperature. Soon, after the washing process, the reclaimed CFPAC was oven dried at 105 °C to reuse it for next cycle. The procedure was repeated for 3–4 cycles (Nirmala et al. 2021; Liadi et al. 2020; Sriramoju et al. 2021). During the investigation, the change in the percentage desorption of pollutant (3) and reusability of CFPAC was evaluated (Nguyen et al. 2016).

$$\%Desorption = \left(\frac{C_{ads} - C_{ds}}{C_{ads}}\right)100 \quad (3)$$

In the above equation, C_{ads} is concentration of pollutant in solid phase at equilibrium (mg/L), C_{ds} is concentration of pollutant desorbed after equilibrium (mg/L).

Analysis of phenol and 2,4-DCP in binary solution

The concentrations of phenol and 2,4-DCP in the bi-solute state were investigated using a UV–Vis spectrophotometer. The estimation method adhered closely to the procedure detailed by Khan and Leong (Khan et al. 1997; Leong et al. 2017). In order to improve the accurateness and precision of method, initially phenol and 2,4-DCP were transformed to their molecular forms via acidification with 1 N HCl solution for both the blank and binary samples of phenol and 2,4-DCP. The quantity of both pollutants in the binary mixture was determined based on absorbance relative to the λ_{max} of phenol and 2,4-DCP at 270 and 283 nm, respectively. Further, the individual concentrations of phenol and 2,4-DCP were subsequently calculated from the equations (4) and (5) which were later substituted with the measured absorbance values of the sample and solved simultaneously.

$$A_{270} = \varepsilon_{11}C_1b + \varepsilon_{12}C_2b \quad (4)$$

$$A_{283} = \varepsilon_{21}C_1b + \varepsilon_{22}C_2b \quad (5)$$

In the above equations, A_{270} and A_{283} denote absorbance at λ_{max} and C_1 and C_2 are the concentrations of phenol and 2,4-DCP, respectively. Further, b is the non-variable path length of sample fixed at 1 cm. Then the ε_{11} and ε_{12} correspond to the molar extinction coefficients of phenol and 2,4-DCP at λ_{max} of 270 nm. Further, ε_{21} and ε_{22} represent the molar extinction coefficients of phenol and 2,4-DCP at λ_{max} of 283 nm. These coefficients were initially acquired from the standard calibration plot of phenol and 2,4-DCP at each λ_{max}. Their values were 0.0151 and 0.0051 L/mg cm with respect to ε_{11} and ε_{12} and 0.0013 and 0.0122 L/mg cm with respect to ε_{21} and ε_{22}.

Characterization of CFPAC

The CFPAC and used adsorbent were characterized using sophisticated techniques such as XRD to comprehend amorphous nature of carbon material (2θ ranging between 5–70°), FTIR to identify functional groups (scanning in the range 4000–400 cm^{-1}), FE-SEM-EDS to obtain magnified images and elemental composition of CFPAC (Gama et al. 2022; Liu et al. 2021; Dong et al. 2021). Further XPS was also performed to obtain survey spectrum and quantify surface electron binding energy of CFPAC and used adsorbent. The surface area: 1146 m^2/g and pore volume: 0.8628 m^3/g of CFPAC are reported elsewhere (Patil et al. 2024).

Modelling of binary experimental data

Binary adsorption was modelled using different binary isotherm models such as extended Langmuir, modified Langmuir, modified Freundlich, non-modified and modified Redlich–Peterson (RP) model (Andriantsiferana et al. 2013; Villar da Gama et al. 2018; Aksu and Akpinar 2001). The details of the isotherms are given in Table 1.

In the above equations, i and j represent each component of a binary matrix, $q_{e,i}$ and $q_{m,i}$ represent adsorption capacity and maximum adsorption capacity of component "i" in presence of "j". $C_{e,i}$ represents equilibrium concentration of component "i". $k_{l,i}$ and $\eta_{l,i}$ are constants from non-modified Langmuir model at equilibrium. $k_{f,i}$, x_i, y_i and z_i are correlative constants from extended Freundlich model. $k_{R,i}$, $a_{R,i}$ are constants from modified RP model at equilibrium.

Table 1 Different multicomponent isotherm models its constants

Binary isotherm model	Nonlinear forms	Model constants	References
Extended Langmuir model	$q_{e,i} = q_{m,i}\frac{k_{l,i}C_{e,i}}{1+\sum_{i=1}^{2} k_{l,i}C_{e,i}}$	$k_{l,i}, q_{m,i}k_{l,j}$	Gupta and Balomajumder (2015)
Modified Langmuir model	$q_{e,i} = q_{m,i}\frac{k_{l,i}\left(C_{e,i}/\eta_{l,i}\right)}{1+\sum_{i=1}^{2} k_{l,i}\left(C_{e,i}/\eta_{l,i}\right)}$	$k_{l,i}, n_{l,i}, n_{l,j}$	Nguyen et al. (2016)
Extended Freundlich model	$q_{e,i} = \frac{k_{f,i}C_{e,i}^{(n_i+x_i)}}{C_{e,i}^{x_i}+y_i C_{e,j}^{z_i}}$	$k_f, n_i\, x_i, y_i, z_i$	Aksu and Akpinar (2001)
Non-Modified RP model	$q_{e,i} = \frac{k_{R,i}(C_{e,i})}{1+\sum_{i=1}^{2} a_{R,i}(C_{e,i})^{\beta,i}}$	$k_{R,i}, a_{R,i}\,\beta_i$	Gaikwad and Balomajumder (2017)
Modified RP model	$q_{e,i} = \frac{k_{R,i}\left(C_{e,i}/\eta_{R,i}\right)}{1+\sum_{j=1}^{2} a_{R,j}\left(C_{e,j}/\eta_{R,j}\right)^{\beta,j}}$	$k_{R,i}, \eta_{R,i}a_{R,i}, \beta, j, \eta_{R,j}$	Patil et al. (2023)

$$R^2 = 1 - \frac{\sum_{i=1}^{n}\left(q_{exp} - q_{pred}\right)^2}{\sum_{i=1}^{n}\left(q_{exp} - \overline{q_{e,avg}}\right)^2} \tag{6}$$

$$SSE = \sum_{i=1}^{n}\left(q_{exp} - q_{pred}\right)^2 \tag{7}$$

$$MPSD = 100\sqrt{\frac{1}{N-p}\sum_{I=1}^{p}\left(\frac{q_{exp,i} - q_{pred,i}}{q_{exp,i}}\right)^2} \tag{8}$$

The data obtained from the experiments were fitted to all the models by minimizing error functions such as sum of squares error (SSE) and Marquardt's percent standard deviation (MPSD) to obtain model constants $k_{l,i}$, $q_{m,i}$, $\eta_{l,i}$, $\eta_{l,j}$, x_i, y_i z_i, $\eta_{R,i}$, $\eta_{R,j}$ (El-Naas et al. 2017; Anumasahun et al. 2023; Agarwal et al. 2013). In the above equations (6), (7) and (8), q_{exp} represents experimental adsorption capacity (mg/g), q_{pred} is calculated adsorption capacity (mg/g), $\overline{q_{exp,avg}}$ represents average of adsorption capacities (mg/g), N shows set of observation in the isotherm investigation, p is number of parameters in the model that are quantified.

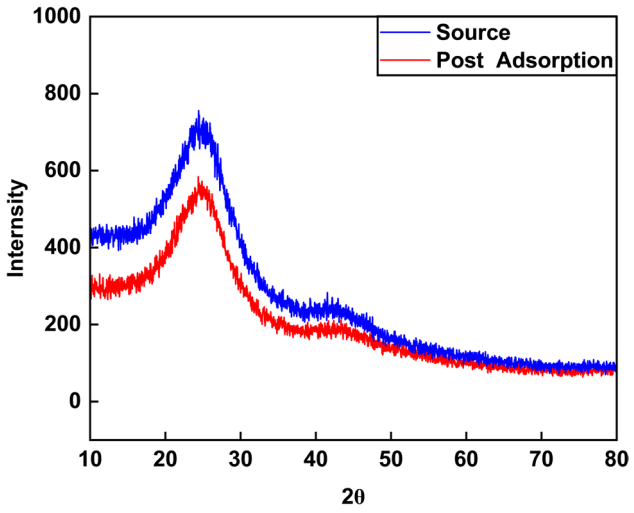


Fig. 1 XRD spectra of CFPAC of before and after adsorption of phenol and 2,4-DCP

Interaction mechanisms and factors

The present investigations into the competitive adsorption of binary pollutants incorporate two potential mechanisms. The fundamental principle underlying these mechanisms involves examining the adsorption capacity for component "i" single system $\left(q_{e,i}\right)_s$ and adsorption capacity for component "i" binary system $\left(q_{e,i}\right)_b$. The ratio of adsorption capacity

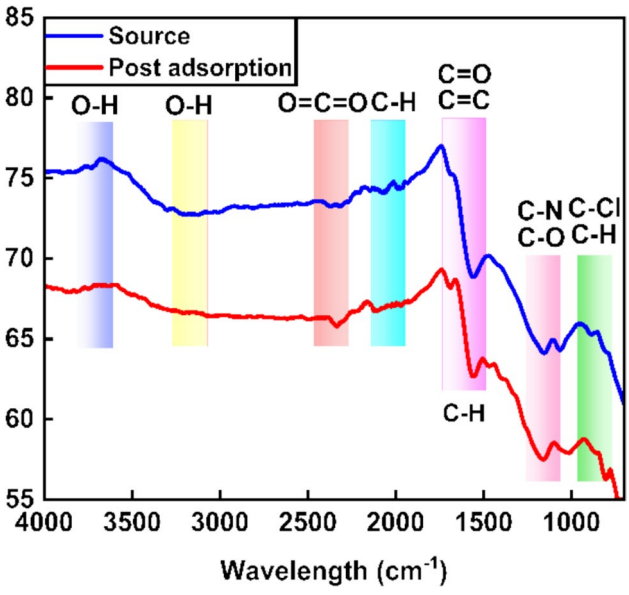


Fig. 2 FTIR spectra of CFPAC of before and after adsorption of phenol and 2,4-DCP

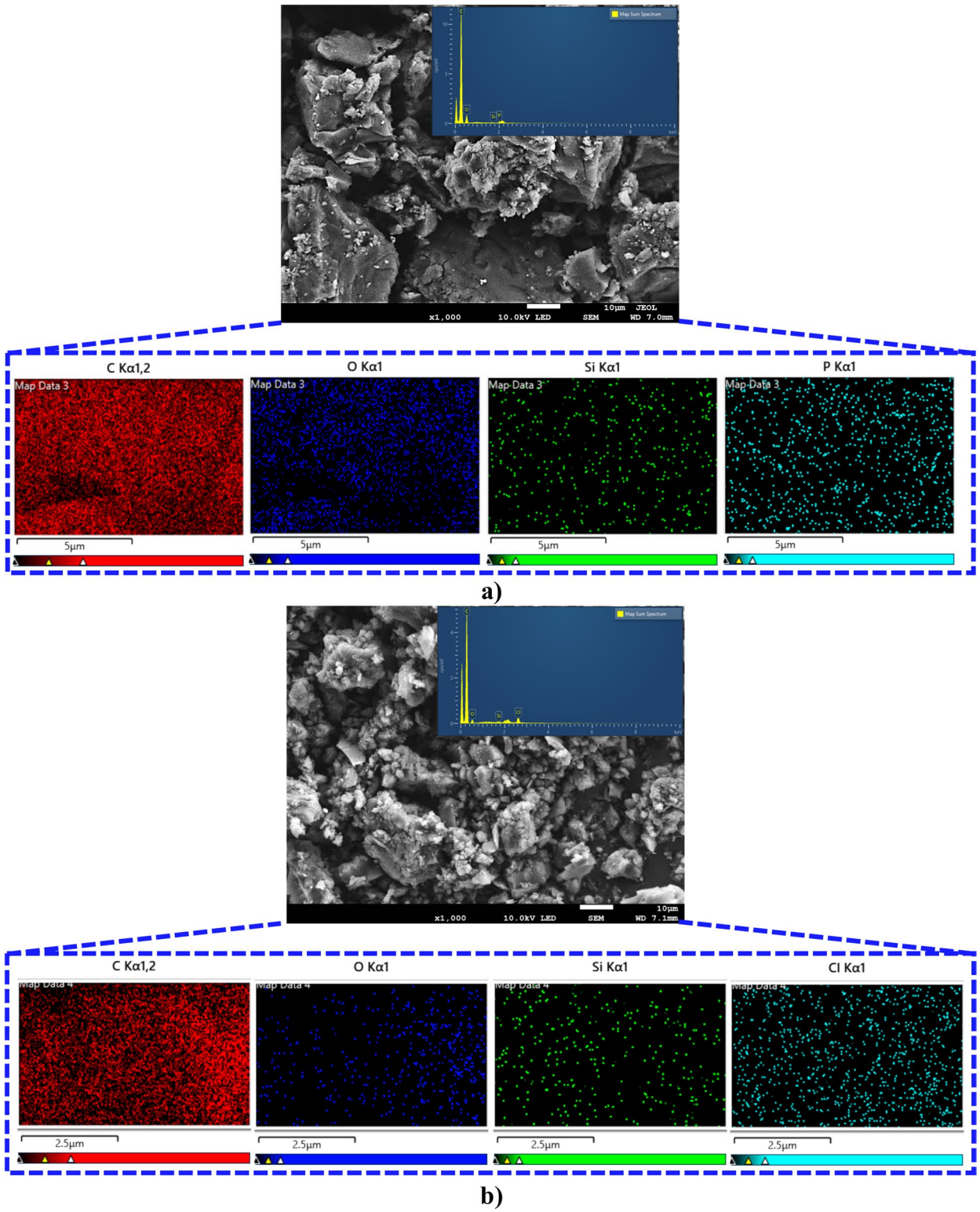


Fig. 3 Magnified (1 K) FE-SEM images, elemental mapping of CFPAC (**a**) before and (**b**) after adsorption of phenol and 2,4-DCP

of a pollutant of in binary solution to its adsorption capacity in individual form is defined as adsorption ratio "$R_{q,i}$", and this fraction value is much significant in identifying different interactions. Further, the comparison of mono-component experimental adsorption capacity $\left(q_{exp,i}\right)_s$ with binary

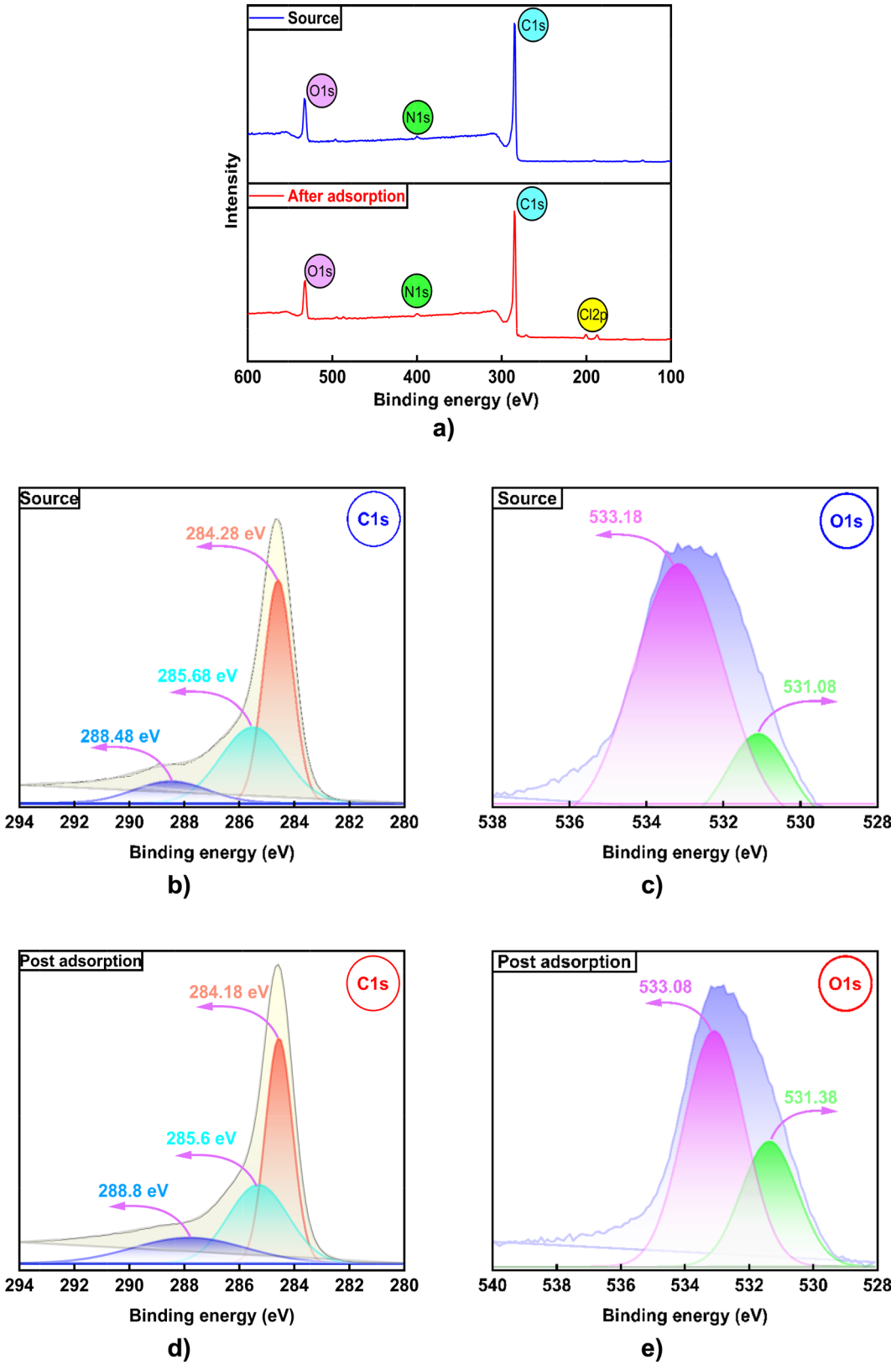


Fig. 4 XPS survey spectra (**a**) C1s deconvoluted speaks of source, post-adsorption (**b**, **d**), O1s deconvoluted peaks of source, post-adsorption (**c**, **e**)

experimental adsorption capacity $\left(q_{exp,i}\right)_b$ can be represent by plotting graph of $\left(q_{exp,i}\right)_s$ vs. $\left(q_{exp,i}\right)_b$.

Synergistic interaction

This is particular interaction in bi-solute adsorption systems, where the presence of one solute increases the adsorption capacity of another (Singanodi et al. 2023; Xie et al. 2022). This interaction can be represented as adsorption capacity ratio ($R_{q,i}$). In this case, the $R_{q,i}$ of $\left(q_{e,i}\right)_b$ and $\left(q_{e,i}\right)_s$ is always greater than 1. Mathematically, it can be represented as below

$$R_{q,i} = \frac{\left(q_{e,i}\right)_b}{\left(q_{e,i}\right)_s} > 1 \tag{9}$$

Antagonistic interaction

This interaction is characterized in binary adsorption systems, wherein the adsorption capacity of a pollutant decreases when it is present alongside another pollutant (Meng, Zhang, and Zhang 2008; Shahbazi, Marnani, and Salahshoor 2019). Additionally, the $R_{q,i}$ of $\left(q_{e,i}\right)_b$ and $\left(q_{e,i}\right)_s$ is observed to be less than 1. The antagonistic interaction is mathematically represented as (10)

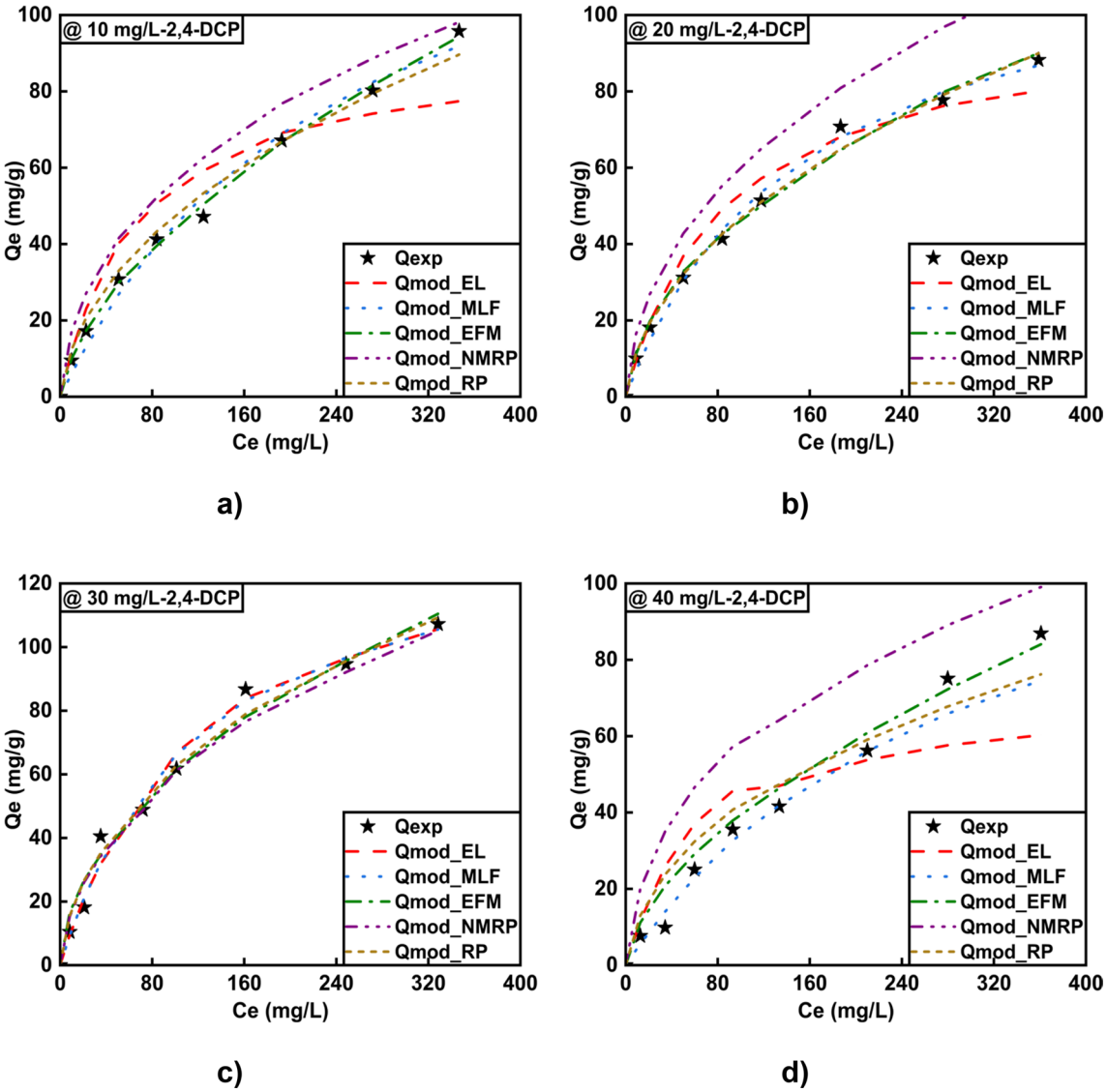


Fig. 5 Comparison of experimental and model data of phenol adsorption at (**a**) 10 mg/L, (**b**)20 mg/L, (**c**) 30 mg/L and (**d**) 40 mg/L concentration of 2,4-DCP

Table 2 Multicomponent isotherm parameter values for the binary adsorption of phenol

Multicomponent models	Parameters	For varying 2,4-DCP in mg/L			
		10	20	30	40
Extended Langmuir	q_{mi} (mg/g)	191.01	164.63	195.15	150
	R^2	0.885	0.964	0.985	0.73
	MPSD	22.97	11.28	10.93	65.35
Modified Langmuir model	n_j	1.930	1.509	0.884	2.70
	n_i	25.03	2.656	1.745	12.5
	R^2	0.984	0.991	0.985	0.95
	MPSD	16.79	13.20	10.95	19.64
Extended Freundlich model	x_i	1.077	2.004	0.502	0.26
	y_i	6.777	32.69	0.166	1.9
	z_i	0.843	2.13	0.851	0.12
	R^2	0.997	0.990	0.973	0.96
	MPSD	5.71	10.44	44.55	70.69
Non-Modified RP model	R^2	0.876	0.735	0.972	0.474
	MPSD	40.21	36.98	23.72	115.99
Modified RP model	n_{ij}	1.852	1.90	0.99	2.11
	n_{ii}	10	6.44	1.34	3
	R^2	0.984	0.991	0.977	0.912
	MPSD	14.02	6.492	24.85	57.84

$$R_{qi} = \frac{(q_{e,i})_b}{(q_{e,i})_s} < 1 \tag{10}$$

Non-Interaction

According to the definition, it is a type of interaction in which there is no significant change in the adsorption capacity of a pollutant when associated with another pollutant (Yadav et al. 2021; Patil et al. 2023) which also means that ratio $(q_{e,i})_b$ and $(q_{e,i})_s$ approaches unity. The equation (11) corresponds to non-interaction form

$$R_{qi} = \frac{(q_{e,i})_b}{(q_{e,i})_s} = 1 \tag{11}$$

P-factor (P_{fi})

It can be defined as the "ratio of the adsorption capacity of a pollutant in a mono-component system to the adsorption capacity in a binary solution". It assesses data pertaining to single-component equilibrium in relation to the binary component. It also enables the comprehension of competitive adsorption dynamics among the components present in a binary solution. The factor additionally elucidates the mechanism by which second element in a binary solution hinders the adsorption of element one. The expression is mathematically represented as in Eq. (12)

$$P_{fi} = \frac{(q_{e,i})_s}{(q_{e,i})_b} \tag{12}$$

The value of $P_{fi} > 1$, implies the adsorption of component i is suppressed and antagonistic interaction in the presence of component j. $P_{fi} < 1$ denotes synergistic type of interaction.

Inhibitory effect

The adsorption of a pollutant may be hindered by another component present in the binary system which can be characterized by the inhibitory effect (ΔIE_i). It is denoted as shown in equation no. (13)

$$\Delta IE_i = \frac{(q_{e,i})_s - (q_{e,i})_b}{(q_{e,i})_s} \tag{13}$$

The positive value of ΔIE_i suggests the adsorption capacity of component "i" is suppressed in the presence of j and the antagonistic interaction is observed in component "i". The negative value indicates enhanced adsorption and synergistic interaction.

Results and discussion

Analysis of XRD spectra of CFPAC

The plot of XRD spectra of source and post-adsorption is illustrated in Fig. 1. The X-ray diffractor meter study was performed to investigate the amorphous/crystalline nature of CFPAC. In both spectra, two distinct peaks are observed: the first at $2\theta \approx 25°$ and the second peak at $2\theta \approx 45°$ (Zheng et al. 2024; Melo et al. 2024). These peaks correspond to a majority of amorphous phase of carbon material and trivial crystalline phase, respectively. It can also be noticed that no sharp peaks have been formed. A similar results were report by (Danish et al. 2022) for the activated carbon prepared using banana trunk.

The red curve (post-adsorption) appears to display slight fluctuations in peak intensities, which could be indication of structural changes or due to the incorporation of adsorbed phenol/2,4-DCP onto the CFPAC. A broader peak was observed in post-adsorption curve as compared to the one obtained in source, suggesting either a decrease in crystallinity or the formation of smaller crystallites after adsorption of phenolic pollutants (Melo et al. 2024). The drop in the peak intensity after adsorption was also owing to partial surface coverage by contaminants, directing a decline in diffraction signals (Kaszkur et al. 2014; Namasivayam and Kavitha

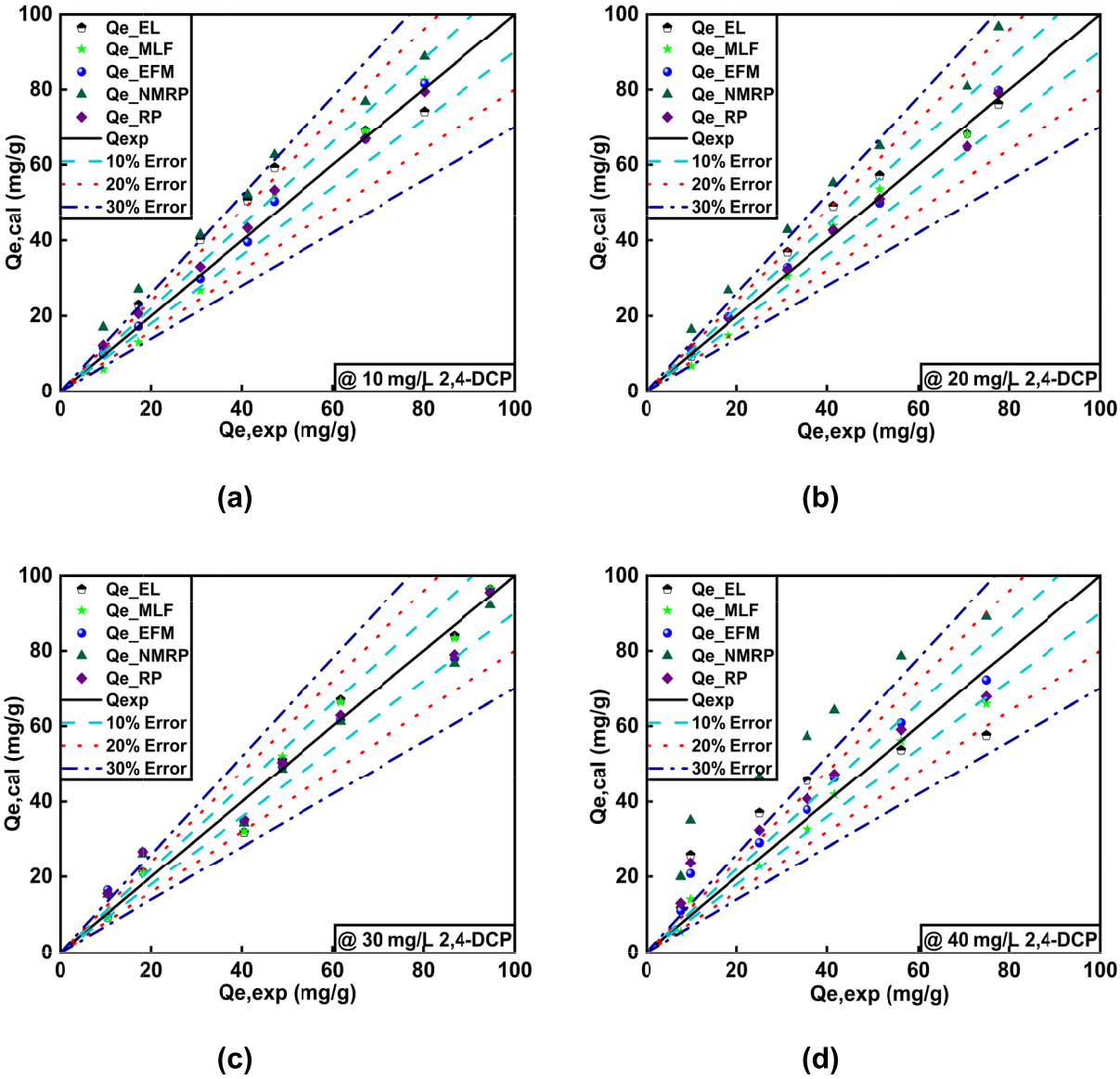


Fig. 6 Parity plot for comparison of experimental and model data of phenol adsorption in binary adsorption system

2006). The result presented in Fig. 1 also demonstrate that the binary adsorption of phenol and 2,4-DCP did not alter the structural space of the CFPAC (Haro et al. 2021).

Analysis of FTIR Spectra of CFPAC

The FTIR spectroscopy of CFPAC before adsorption (blue coloured) and after adsorption (red colour) is shown in Fig. 2. The spectra of CFPAC illustrate that there are multiple functional elements that are being detected. Two peaks due to the O–H stretching of adsorbed water, alcohols and carboxyl's approximately at 3140 and 3670 cm^{-1} in the region between 3000–3790 cm^{-1} are observed. A similar observation reported by (Mishra et al. 2022) for banana peel derived activated carbon. A shift in the peaks to 3150 and 3593 cm^{-1}can also be noted.

Further, the peaks responsible for alkanes and alkyls groups were found between 2700 and 3000 cm^{-1} (Pei et al. 2023). However, after adsorption meagre stretching of C-H bonds can be observed (Vohra et al. 2023). The small peak at 2000 cm^{-1} illustrates C–O–C stretching, and the peak at 1470 cm^{-1} is ascribed to stretching of C = C aromatic rings (Mourão et al. 2024). A trivial shift can be observed in both the peaks after adsorption of phenol/2,4-DCP. In addition, the trace of bands between 1000 and 1200 cm^{-1} signifies stretching C-O bonds. While peak between 700–750 cm^{-1}

Table 3 Comparison of single and binary adsorption parameters of phenol in presence of 2,4-DCP

$C_{o,PH}$ (mg/L)	$C_{o,DCP}$ (mg/L)	$Q_{e,PH}$ (mg/g)	$Q_{e,DCP}$ (mg/g)	$Ad_{PH\%}$	R_{qi}	P_{fi}	ΔIE_i	Type of interaction
25	0	12.77	0	81.75	1.0	1.0	1.0	No Interaction
50	0	22.85	0	73.12	1.0	1.0	1.0	
100	0	38.64	0	61.83	1.0	1.0	1.0	
150	0	52.66	0	56.17	1.0	1.0	1.0	
200	0	66.30	0	53.04	1.0	1.0	1.0	
300	0	88.18	0	47.03	1.0	1.0	1.0	
400	0	108.67	0	43.47	1.0	1.0	1.0	
500	0	118.75	0	38.00	1.0	1.0	1.0	
25	10	9.5	5.062	60.710	0.744	1.346	0.257	Antagonistic Interaction
50	10	17.2	3.719	55.030	0.753	1.329	0.247	
100	10	30.8	1.136	49.231	0.797	1.256	0.204	
150	10	41.2	1.079	43.984	0.782	1.277	0.217	
200	10	47.2	1.02	37.722	0.712	1.406	0.289	
300	10	67.1	0.974	35.799	0.761	1.314	0.239	
400	10	80.3	0.925	32.101	0.739	1.354	0.262	
500	10	95.8	0.879	30.651	0.807	1.240	0.193	
25	20	10.0	11.661	64.083	0.783	1.275	0.216	Antagonistic Interaction
50	20	18.1	10.896	58.030	0.792	1.260	0.206	
100	20	31.2	9.057	49.885	0.807	1.239	0.193	
150	20	41.4	6.767	44.126	0.786	1.273	0.214	
200	20	51.4	4.334	41.132	0.775	1.290	0.225	
300	20	70.8	0.031	37.744	0.803	1.246	0.197	
400	20	77.7	0.025	31.084	0.715	1.398	0.285	
500	20	88.2	0.012	28.231	0.743	1.346	0.257	
25	30	10.4	17.665	66.864	0.814	1.222	0.182	Antagonistic Interaction
50	30	18.2	16.477	58.107	0.796	1.258	0.205	
100	30	40.5	14.928	64.793	1.048	0.954	0.048	
150	30	48.9	11.002	52.110	0.929	1.078	0.072	
200	30	61.8	12.552	49.408	0.932	1.074	0.068	
300	30	86.7	9.194	46.252	0.983	1.017	0.017	
400	30	94.7	2.221	37.870	0.871	1.148	0.129	
500	30	107.2	1.911	34.320	0.903	1.107	0.097	
25	40	7.7	23.709	49.112	0.603	1.664	0.399	Antagonistic Interaction
50	40	9.8	22.521	31.479	0.429	2.323	0.569	
100	40	25.0	20.661	40.059	0.647	1.543	0.352	
150	40	35.5	17.665	37.909	0.674	1.482	0.325	
200	40	41.6	9.762	33.284	0.627	1.594	0.372	
300	40	56.2	1.498	29.980	0.637	1.569	0.363	
400	40	75.1	1.123	30.030	0.691	1.448	0.309	
500	40	86.9	0.955	27.811	0.732	1.366	0.268	

represents stretching of aromatic C-H, however an intense peak at 780 cm^{-1}representing C–Cl bond is also found which is due to adsorption of 2,4-DCP molecules (Cui et al. 2017). These distinct functional groups can play a significant role in removal of phenolic pollutants.

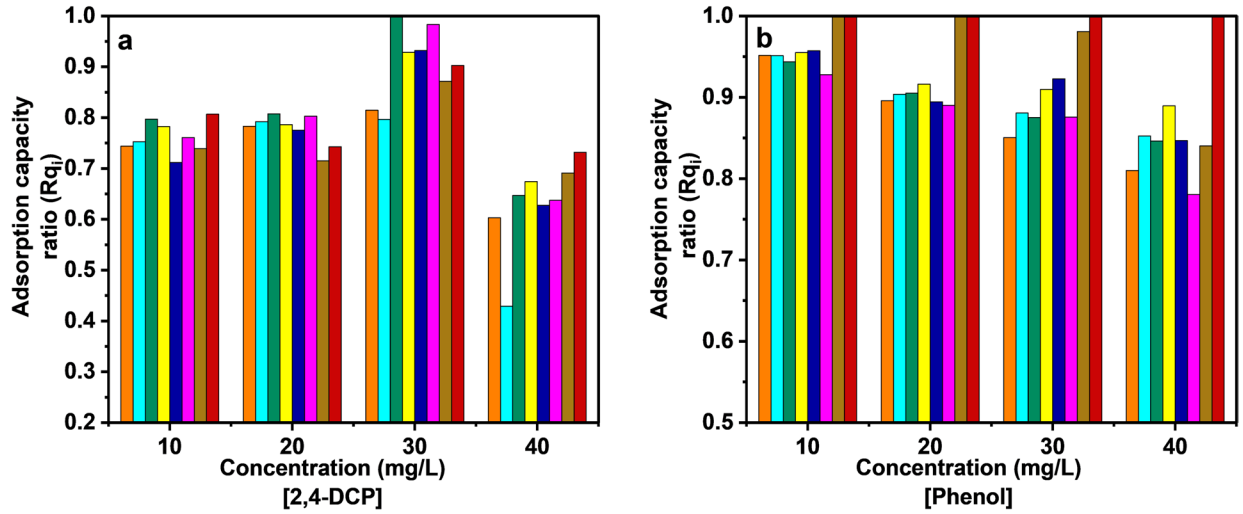


Fig. 7 R_{qi} plot of (**a**) phenol and (**b**) 2,4-DCP adsorption in binary adsorption system

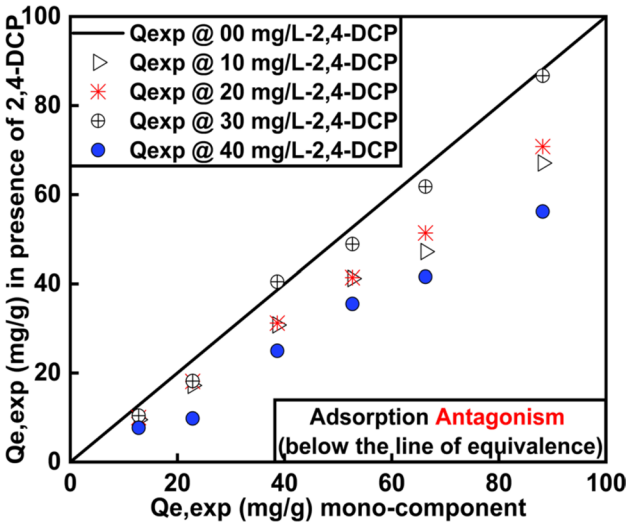


Fig. 8 Comparison of mono-component experimental values with multicomponent experimental values in presence of 2,4-DCP

Analysis of FE-SEM-EDS of CFPAC

The structural properties of CFPAC and used adsorbent were investigated by FE-SEM at 1 K magnification as shown in Fig. 3 (a) & (b). Large number of uneven pores and apertures with roughness on surface formed due to the activation using H_3PO_4 can be observed. The material can facilitate the adsorption of phenol and 2,4-DCP (Tao et al. 2019; Mishra et al. 2022). A comparable result was also testified by Abdulrahman (Abdulrahman et al. 2023). The elemental mapping of CFPAC shows uniform distribution of carbon (C) alongside least percentage of oxygen, silica and phosphorus (O, Si, P) depicting pure form of carbon. Figure 3 (b) illustrates diminished image (1 K) post-adsorption of phenol/2,4-DCP molecules onto activated carbon. From the image, a significant change in surface as compared to pre-adsorbed state can be visualized.

A drop in size and porosity of the material was due to the adsorption of phenols. The size of pores was found to be diminished as observed from Fig. 3 (b). Furthermore, from the elemental mapping, a noticeable rise in the distribution of carbon and oxygen can be observed which was mainly due to oxygen containing functional groups of phenol/2,4-DCP that got attached to CFPAC (Ayoob et al. 2024). In addition, the presence of chlorine clearly depicts adsorption of 2,4-DCP as well.

Analysis of XPS spectra of CFPAC

XPS of source and post-adsorption was executed to examine the elemental configuration and chemical state. The complete XPS survey spectra of the source and used adsorbent showed different peaks linked to C1s, O1s, N1s and Cl2p, as shown in Fig. 4. It could be found that the peaks of C1s and O1s in the XPS spectra were declined post-adsorption, and a new peak with 200.08 eV detected, which corresponds to chlorine element. The peak Cl2p is a signal associated with the adsorption of 2,4-DCP from the binary solution. Similar results have also been reported for the adsorption of 2,4-DCP on *Populus Nigra* (G. Zhang et al. 2024).

Further, after the deconvolution of C1s species, three distinct peaks, as illustrated in Fig. 4 **(b),** can be observed. A superior signal at 284.28 eV is related to C–C and C = C, showing the presence of carbon. Then, two smaller signals at 285.68 and 288.48 eV demonstrate the presence of oxygen-holding groups, i.e. C-O and C = O, respectively (Luo et al. 2019)**.** Similar outcomes were also reported for the adsorption of phenolic pollutants over coconut shell-derived activated carbon (M. Li et al. 2022a, b). A shift

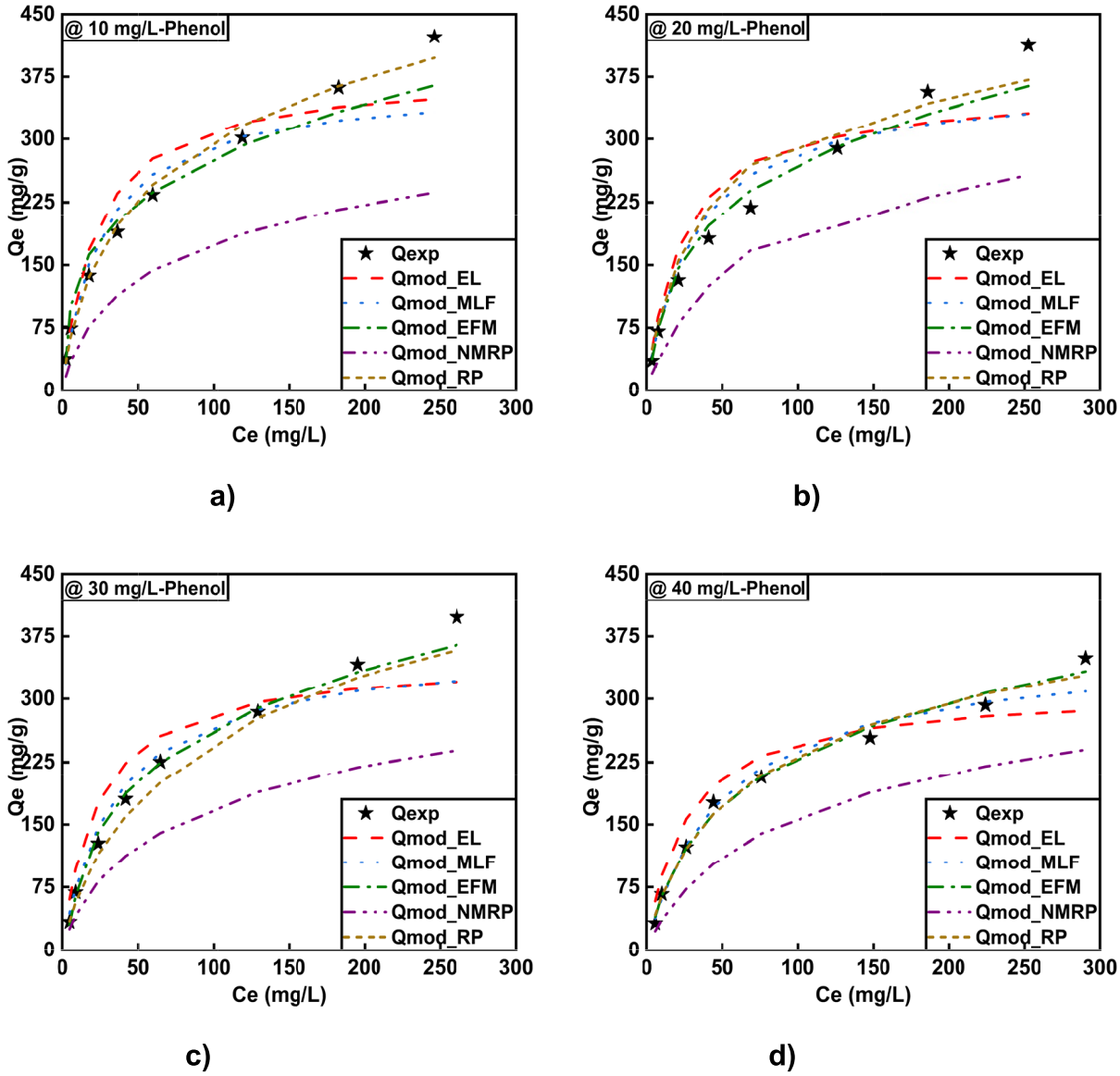


Fig. 9 Comparison of experimental and model data of 2,4-DCP adsorption at (**a**) 10 mg/L, (**b**) 20 mg/L, (**c**) 30 mg/L and (**d**) 40 mg/L concentration of phenol

of the above-mentioned binding energies to 284.18, 285.60 and 288.80 eV, respectively, as shown in Fig. 4 **(c)**, can be distinguished owing to hydrogen bonding of oxygen-holding groups present in the CFPAC (Zhaoyang Li et al. 2024) with phenol/2,4-DCP.

In addition, the deconvolution analysis of the O1s species returned two peaks with binding energies of 531.08 and 533.18 eV, as shown in Fig. 4 **(d)**, corresponding to C = O and C–OH (Cho et al. 2022; K. Li et al. 2019a, b). However, a shift in the O1s signals to 531.38 and 533.08 eV, respectively, as presented in Fig. 4 **(e)**, designates adsorption of both the pollutants, which is likely due to hydrogen bonding/π-π stacking (Zhaoyang Li et al. 2022a, b).

Multicomponent adsorption

Analysis of binary batch studies of phenol with 2,4-DCP

Binary adsorption was carried out for phenol in the presence of different concentrations of 2,4-DCP.

Table 4 Multicomponent isotherm parameter values for the binary adsorption of 2,4-DCP

Multicomponent models	Parameters	For varying phenol in mg/L			
		10	20	30	40
Extended Langmuir model	q_{mi} (mg/g)	398.52	371.21	366.09	326.54
	R^2	0.912	0.878	0.883	0.910
	MPSD	15.11	24.71	36.36	33.65
Modified Langmuir model	n_J	1.14	1.35	1.58	2.156
	n_i	6.5	3.5	3.1	3.00
	R^2	0.917	0.911	0.933	0.974
	MPSD	12.92	13.96	14.93	8.78
Extended Freundlich model	x_i	3.156	1.41	1.638	1.214
	y_i	1.89	2.5	3.5	0.087
	z_i	1.3	0.563	0.84	1.539
	R^2	0.955	0.968	0.987	0.989
	MPSD	25.33	13.28	10.63	15.26
Non-Modified RP model	R^2	0.320	0.533	0.451	0.586
	MPSD	44.51	37.01	36.08	34.83
Modified RP model	η_j	0.019	0.26	0.0169	0.317
	η_i	0.001	0.45	0.0046	0.366
	R^2	0.991	0.945	0.972	0.986
	MPSD	7.573	19.96	9.93	11.83

Further, the obtained experimental data were modelled using multicomponent adsorption models (Zichao Li et al. 2019a, b). These predicted values were compared with experimental values by plotting C_e vs. q_e. The details can be observed in Fig. 5 (a) to (d). The parameters R^2 and MPSD pertaining to the multicomponent adsorption model for phenol are shown in Table 2. It was evident from the higher value of MPSD that the non-modified RP model showed a poor fit in most of the cases. Meanwhile, it was also established based on R^2 that the modified Langmuir model adequately fitted the experimental data (Singh and Balomajumder 2016).

Further, it was observed that the uptake of phenol got reduced from 191.011 mg/g to 150 mg/g, corresponding to an increase in 2,4-DCP concentration from 10 to 40 mg/L.

Furthermore, binary adsorption data were also examined by evaluating the adsorbed amounts of phenol and 2,4-DCP as predicted by multicomponent models, q_{cal}, vs. the experimental value, q_{exp} by means of parity plots (Sukpreabprom et al. 2015). The graph of. q_{exp} vs. q_{cal} for the phenol, where 2,4-DCP is varied from 10 to 40 mg/L in the system, is shown in Fig. 6 (a) to (d).

The plot consists of seven lines, a dark continuous line specifies reference line wherein $q_{cal.} = q_{exp}$. Further, 3 dotted lines above the centre line are shown where $q_{cal} = 1.1*q_{exp}$, $q_{cal} = 1.2*q_{exp}$ and $q_{cal} = 1.3*q_{exp}$ indicate overestimation by 10%, 20% and 30%, respectively. Furthermore, 3 dotted lines below the centre line where $q_{cal} = 0.9*q_{exp}$, $q_{cal} = 0.8*q_{exp}$ and $q_{cal} = 0.7*q_{exp}$ denote under estimation by 10%, 20% and 30%, respectively. In addition, it can also be deduced from Fig. 6 that, despite the better fit to experimental data, the modelled values fall in the overestimated region.

The type of interaction in binary adsorption of phenol and 2,4-DCP was quantified using adsorption capacity and removal efficiency (Table 3). It can be observed that the mono-component adsorption capacity of phenol was 12.77 mg/g; however, the adsorption ability in the presence of 2,4-DCP was dropped to 7.7 mg/g. Further, the respective removal efficacy of CFPAC for 25 mg/L of phenol drastically reduced from 81.75% to 49.11% when 2,4-DCP was varied from 10 to 40 mg/L. A similar observation was also noted for other concentrations of phenol, thus suggesting an antagonistic interaction in the adsorption process was prominent.

Further, it is also possible to quantify the interaction by means of, R_{qi}, $P_{fi\ i}$ and ΔIE_i (discussed under interaction mechanism and factors). The results of R_{qi} for phenol are plotted in Fig. 7 (a). It is possible to compare mono-component experimental adsorption capacity $(q_{exp,i})_s$ with binary experimental adsorption capacity $(q_{exp,i})_b$ and can be represent by plotting graph of $(q_{exp,i})_s$ vs. $(q_{exp,i})_b$. The centre dark line represents adsorption capacity in single state, and other symbol represents adsorption capacity in binary state. If the experimental values in binary state are above the line, it would be called as synergism and below the line represents antagonism (Y. Zhang et al. 2019). In the present case, all the values pertaining to adsorption capacity of phenol in presence of 2,4-DCP fall below the dark line thus indicating antagonism in binary state (Fig. 8). The adsorption ratio

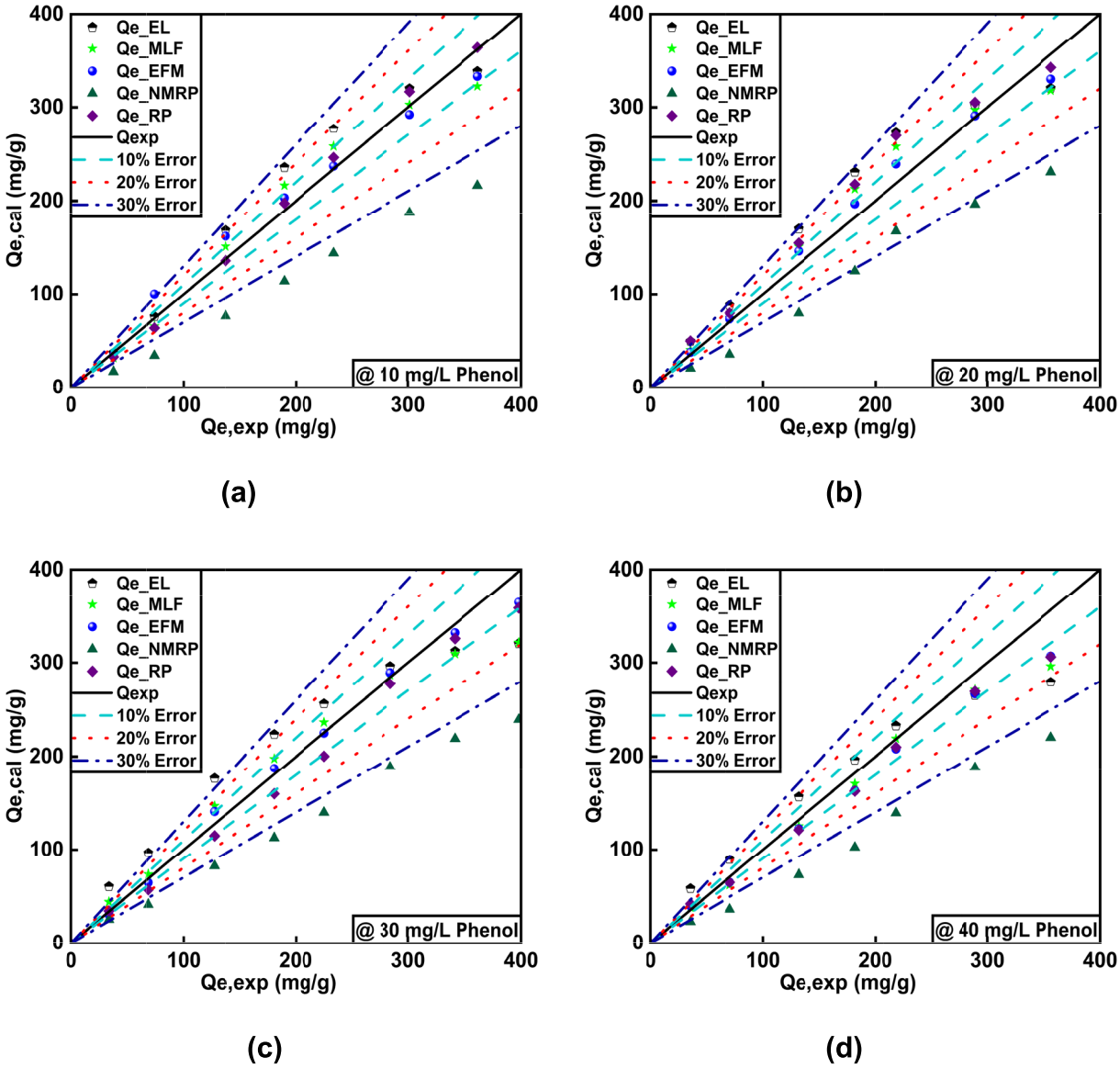


Fig. 10 Parity plot for comparison of experimental and model data of 2,4-DCP adsorption in binary adsorption system

$R_{qi} = 1$ illustrates non-interaction, $R_{qi} > 1$ depicts enhanced adsorption of pollutant i when coexist with other pollutant, $R_{qi} < 1$ indicates suppressed adsorption of pollutant i by other pollutant.

Herein, it can be observed from the plot and from the range of values evaluated for the obtained R_{qi} were less than 1, thus depicting the adsorption capacity of phenol was suppressed in presence of 2,4-DCP and indicating antagonistic interaction. Furthermore, $P_{fi} < 1$ illustrates cooperative interaction and $P_{fi} > 1$ competitive interaction. In the present case, the average of $P_{fi} > 1$ for all the cases illustrates antagonistic interaction in the presence of 2,4-DCP. In addition, $\Delta IE_i > 0$ indicates the adsorption ability of phenol was suppressed when coexisted with 2,4-DCP.

Analysis of binary batch studies of 2,4-DCP with phenol

The binary adsorption investigation was carried out for 2,4-DCP in the presence of different concentrations of phenol and modelled using multicomponent adsorption models (Ortiz-Martínez et al. 2016). The calculated values were compared with experimental values by plotting C_e vs. q_e. The pictorial representation is shown in Fig. 9 (a) to (d).

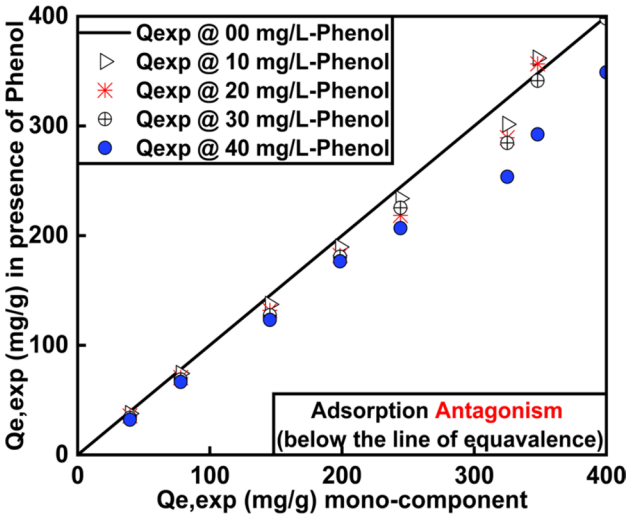


Fig. 11 Comparison of mono-component experimental values with multicomponent experimental values in presence of phenol

All the model parameters and error functions related to the multicomponent adsorption isotherm for 2,4-DCP are listed in Table 4. In the case of 2,4-DCP as well, the non-modified RP model showed an insignificant fit with a greater deviation in MPSD value. Meanwhile, based on higher R^2 and lower MPSD values it was established that the modified Langmuir and modified RP model nearly fitted the experimental data (Nguyen et al. 2016).

Further, it was observed that the uptake capacity of 2,4-DCP was reduced from 398.52 mg/g to 326.54 mg/g, corresponding to a rise in phenol load from 10 to 40 mg/L. This drop suggests competitive adsorption, where phenol and 2,4-DCP interact with active sites of CFPAC. The FE-SEM results as shown in Fig. 3 reveal a high density of mesopores while the binding energies as mentioned Fig. 4 (Kumar et al. 2019) confirm surface heterogeneity.

These findings also confirm that CFPAC sites are energetically diverse, influencing the adsorption behaviour. Consequently, the binary adsorption of 2,4-DCP and phenol can be attributed to surface energetic heterogeneity, where competition for the adsorption sites governed by affinities and energy distribution.

Furthermore, in this case also, binary adsorption data were also examined by evaluating the adsorbed amounts of 2,4-DCP and phenol as predicted by multicomponent models, q_{cal}, vs. the experimental value, q_{exp} by means of parity plots.

The plot of q_{exp} vs. q_{cal} for the 2,4-DCP where phenol was varied from 10 to 40 mg/L in the system is shown in Fig. 10 (a) to (d). The plot shows the extent of variation of estimated model data, which ranges from $q_{cal} = 0.7*q_{exp}$ to $q_{cal} = 1.3*q_{exp}$ thus covering a region from under to overestimation. Figure 10 shows that regardless of the better fit of experimental values with all the models, the calculated data fall in the region of ± 20% error margin. It was also noted that the non-modified RP model showed significant deviation and was in the underestimated region.

In the case of 2,4-DCP, binary adsorption capacity of 2,4-DCP in presence of phenol was below the equivalence line thus indicating antagonistic behaviour (Fig. 11). Further, the nature of adsorption in binary pollutant adsorption of 2,4-DCP and phenol was also computed by means of adsorption capacity and removal efficiency (Table 5). It can be observed that the adsorption capacity of 2,4-DCP was dropped to 32.1 mg/g from 39.62 mg/g. Further, a significant drop in the removal efficacy of 2,4-DCP from 95.096% to 77.025% in the presence of phenol was also observed. Comparable trends were also noted for other concentrations of 2,4-DCP, illustrating antagonistic interaction.

Further, R_{qi}, $P_{fi\ i}$ and ΔIE_i were quantified to identify the interaction type. The results of R_{qi} for 2,4-DCP are plotted in Fig. 7 (b), which shows that, in most cases where 2,4-DCP coexisted with phenol, the $R_{qi} < 1$ indicating competitive adsorption. Furthermore, the average of $P_{fi} > 1$ and $\Delta IE_i > 0$ indicated the adsorption ability of 2,4-DCP is inhibited when coexisting with phenol in an aqueous solution. From all these investigations, it can also be concluded that 2,4-DCP has more possess greater affinity as compared to phenol towards CFPAC. The better affinity of 2,4-DCP towards CFPAC can be explained from $P_{fi\ i}$ wherein it can be observed that P_{fi} of 2,4-DCP was less than P_{fi} of phenol. Additionally, this could also be due to molecular size, hydrophobicity of 2,4-DCP being higher in contrast to phenol (Xiong et al. 2024).

Analysis of regeneration studies

The potential for regeneration and reusability of adsorbents are critical factors in assessing their viability for commercial utilization. The desorption performance and ability to be reused of the CFPAC were evaluated over the course of four consecutive cycles. As illustrated in Fig. 12**,** the CFPAC usage after every adsorption–desorption cycle remained relatively consistent till the fourth cycle. The data also reveal that the adsorption percentage declined from 57.64% to 39.93% for phenol and from 89.52% to 78.12% for 2,4-DCP, after four cycles. Similar observations were also reported for the desorption of p-chlorophenol and nitrophenol from the surface of modified activated carbon (Suresh et al. 2021). The drop in the efficacy was due to incomplete desorption of phenol and 2,4-DCP from the surface of CFPAC. The adsorbent material also exhibited the capability to be recycled and

Table 5 Comparison of single and binary adsorption parameters of 2,4-DCP in presence of phenol

$C_{o,DCP}$ (mg/L)	$C_{o,PH}$ (mg/L)	$Q_{e,DCP}$ (mg/g)	$Q_{e,PH}$ (mg/g)	$Ad_{DCP\%}$	R_{qi}	P_{fi}	ΔIE_i	Type of interaction
25	0	39.623	0	95.096	1.0	1.0	1.0	Non- Interaction
50	0	78.007	0	93.608	1.0	1.0	1.0	
100	0	145.486	0	87.292	1.0	1.0	1.0	
150	0	198.535	0	79.414	1.0	1.0	1.0	
200	0	244.256	0	73.276	1.0	1.0	1.0	
300	0	325.004	0	65.001	1.0	1.0	1.0	
400	0	348.007	0	52.201	1.0	1.0	1.0	
500	0	332.121	0	39.854	1.0	1.0	1.0	
25	10	37.7	4.586	90.413	0.951	1.052	0.049	Antagonistic Interaction
50	10	74.2	2.318	89.008	0.951	1.052	0.049	
100	10	137.3	2.202	82.397	0.944	1.059	0.056	
150	10	189.6	2.092	75.840	0.955	1.047	0.045	
200	10	233.8	1.987	70.145	0.957	1.045	0.043	
300	10	301.5	1.888	60.303	0.928	1.078	0.072	
400	10	361.8	1.793	54.277	1.040	0.962	0.040	
500	10	423.0	1.704	50.760	1.274	0.785	0.274	
25	20	35.5	11.476	85.124	0.896	1.117	0.105	Antagonistic Interaction
50	20	70.5	3.514	84.628	0.904	1.106	0.096	
100	20	131.7	2.969	79.050	0.905	1.104	0.094	
150	20	181.9	2.052	72.755	0.916	1.092	0.084	
200	20	218.5	0.846	65.558	0.895	1.118	0.105	
300	20	289.3	0.762	57.851	0.890	1.124	0.110	
400	20	356.7	0.690	53.512	1.025	0.975	0.025	
500	20	412.5	0.514	49.504	1.242	0.805	0.242	
25	30	33.7	25.247	80.826	0.851	1.177	0.150	Antagonistic Interaction
50	30	68.7	22.436	82.397	0.881	1.136	0.120	
100	30	127.3	12.919	76.364	0.875	1.143	0.125	
150	30	180.6	1.430	72.231	0.910	1.099	0.090	
200	30	225.4	1.215	67.624	0.923	1.084	0.077	
300	30	284.6	1.033	56.915	0.876	1.142	0.124	
400	30	341.3	0.878	51.198	0.981	1.020	0.019	
500	30	398.1	0.746	47.769	1.199	0.834	0.199	
25	40	32.1	17.604	77.025	0.810	1.235	0.190	Antagonistic Interaction
50	40	66.5	12.327	79.752	0.852	1.174	0.148	
100	40	123.1	11.711	73.884	0.846	1.181	0.154	
150	40	176.6	11.125	70.634	0.890	1.124	0.111	
200	40	206.8	10.569	62.045	0.847	1.181	0.153	
300	40	253.7	10.041	50.744	0.781	1.281	0.219	
400	40	292.4	9.539	43.864	0.840	1.190	0.160	
500	40	348.9	9.062	41.868	1.051	0.952	0.051	

reused for at least four consecutive adsorption–desorption cycles, maintaining a good of adsorption efficiency. It was also found that over 52.86% of adsorbed phenol and 81.95% of adsorbed 2,4-DCP could be desorbed and recovered from the adsorbent surface using 0.1 N NaOH after the fourth cycle. The CFPAC, with its simple and efficient regeneration process and favourable reusability, can serve as a reasonable and effective material for binary removal for phenol and from aqueous media in industrial treatment (Mandal et al. 2021; Kakavandi et al. 2016).

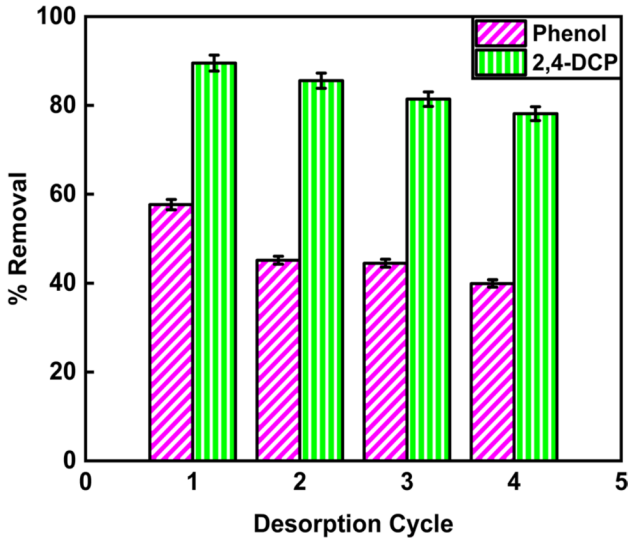


Fig. 12 Reusability of CFPAC over four adsorption–desorption cycle in binary system

Conclusions

In industry, effluents rarely contain a single component; thus, the adsorption system design must be based on multicomponent effluents, making binary investigation a necessity. So, the present investigation delved into characterization of CFPAC post the adsorption of binary pollutants, an experimental and comprehensive study on the adsorptive removal of phenol and 2,4-DCP, which are also recognized as significant environmental pollutants, in binary adsorption system. Additionally, the investigation also involved regeneration of CFPAC in binary adsorption.

The results of characterization of CFPAC by XRD revealed that the adsorption of phenols did not impact the structure surface. The FE-SEM and EDS showed diminished pore size and presence of Cl which indicated adsorption of phenol and 2,4-DCP, respectively. A drop in the intensities of FTIR peaks and the binding energies of C1s and O1s spectra of XPS post-adsorption suggested the interaction between CFPAC and pollutants.

In the multicomponent model, it was possible to determine that, for both pollutants, the non-modified RP model showed a poor result as the model values showed highest average MPSD. Further, it was also established that the modified Langmuir model better explained the binary adsorption with $R^2 > 0.95$ when phenol was considered. However, in case of 2,4-DCP modified RP model, it nearly fitted the experimental data with the least average MPSD. From the binary study, it was revealed that the adsorption capacity of phenolic pollutants significantly subsided when coexisted with other pollutant. Additionally, in the case of phenol for the adsorption of 25 mg/L with 25 mg/L of 2,4-DCP, the adsorption efficacy declined from 81 to 60% and corresponding adsorption capacity reduced to 9.5 mg/g from 12.77 mg/g.

Further, for 25 mg/L of 2,4-DCP, the adsorption efficacy declined from 95 to 90% and the adsorption capacity from 39.6 mg/g to 37 mg/g. In both the cases, it was evident that antagonistic interaction played the key role. It is also important to note that the parity plot used for comparison of experimental and predicted values well contained all the predicted values within least error of 10% with slightly falling in the overestimated region.

The interaction factors used in the investigation, i.e. $R_{qi} < 1$, $P_{fi} > 1$ and $\Delta IE_i > 0$, also denote antagonistic interaction. It was also discovered that after the fourth cycle, the eluent could desorb over 52.86% of the phenol and 81.95% of the 2,4-DCP from the spent CFPAC surface. The model parameters provided insights into material characterization, the adsorption capacity, binary adsorption modelling and interaction factors which would be vital for designing large-scale treatment systems.

Author contribution Mr.Praveengouda Patil conceptualization, methodology, investigation, data curation, validation, formal analysis and modelling. Dr. Gautham Jeppu : project administration and supervision. Ms. Swathi Nayak : data curation, reviewing and modelling. Dr. Chikmagalur Raju Girish :project administration, conceptualization, validation, resources, supervision, proofreading and editing.

Funding Open access funding provided by Manipal Academy of Higher Education, Manipal. The research was not funded by any agencies, and all the experiments were performed in Department of Chemical Engg.

Declarations

Conflict of interest All the authors declare that there is no conflict of interest.

Open Access This article is licensed under a Creative Commons Attribution 4.0 International License, which permits use, sharing, adaptation, distribution and reproduction in any medium or format, as long as you give appropriate credit to the original author(s) and the source, provide a link to the Creative Commons licence, and indicate if changes were made. The images or other third party material in this article are included in the article's Creative Commons licence, unless indicated otherwise in a credit line to the material. If material is not included in the article's Creative Commons licence and your intended use is not permitted by statutory regulation or exceeds the permitted use, you will need to obtain permission directly from the copyright holder. To view a copy of this licence, visit http://creativecommons.org/licenses/by/4.0/.

References

Abdulrahman Mustafa S, Alsarayreh Alanood A, Barno Suondos K. A, Abd Mervat A (2023) Activated carbon from sugarcane as an efficient adsorbent for phenol from petroleum refinery

wastewater: equilibrium, kinetic, and thermodynamic study. Open Eng 13(1):63. https://doi.org/10.1515/eng-2022-0442

Agarwal B, Sengupta P, Balomajumder C (2013) Equilibrium, kinetic and thermodynamic studies of simultaneous co-adsorptive removal of phenol and cyanide using Chitosan. Int J Chem Nucl Mater Metall Eng 7(11):514–521. https://doi.org/10.5281/zenodo.2658356

Aksu Z, Akpinar D (2001) Competitive biosorption of phenol and chromium(VI) from binary mixtures onto dried anaerobic activated sludge. Biochem Eng J 7(3):183–193. https://doi.org/10.1016/S1369-703X(00)00126-1

Andriantsiferana C, Julcour-Lebigue C, Creanga-Manole C, Delmas H, Wilhelm A-M (2013) Competitive adsorption of P-hydroxybenzoic acid and phenol on activated carbon: experimental study and modeling. J Environ Eng 139(3):402–409. https://doi.org/10.1061/(asce)ee.1943-7870.0000600

Anumasahun OV, Akinola AO, Bello OO, Agboola OS, Bello OS (2023) Removal of 2,4-dichlorophenol from aqueous medium using activated carbon prepared from cocoa pod husks. Chem Data Collections 44(January):100997. https://doi.org/10.1016/j.cdc.2023.100997

Ayoob HW, Ali MR, Ala'a AJ, Nabil KT, Raad ZH, Hayder IM (2024) Enhanced adsorption of phenol using graphene oxide-bentonite nanocomposites: synthesis, characterisation, and optimisation. J Mol Liq. https://doi.org/10.1016/j.molliq.2023.123833

Chakraborty N, Mitra R, Pal S, Ganguly R, Acharya K, Minkina T, Sarkar A, Keswani C (2023) Biopesticide consumption in india: insights into the current trends. Agriculture 13(3):557. https://doi.org/10.3390/agriculture13030557

Cho EJ, Chang GL (2022) Adsorption of phenol on kenaf-derived biochar: studies on physicochemical and adsorption characteristics and mechanism. Biomass Conver Biorefinery. https://doi.org/10.1007/s13399-022-03262-x

Cui L, Tianming C, Guixiang Q, Bo X, Yurong M, Mei P, Yang L et al (2017) Renewable material-derived biochars for the efficient removal of 2,4-dichlorophen from aqueous solution: adsorption/desorption mechanisms. BioResources 12(3):4912–25

da Gama V, Maria B, Elisandra G (2018) Mono and binary component adsorption of phenol and cadmium using adsorbent derived from peanut shells. J Clean Prod 201:219–228. https://doi.org/10.1016/j.jclepro.2018.07.291

Danish M, Pin Z, Ziyang L, Ahmad T, Majeed S, Yahya ANA (2022) Preparation and characterization of banana trunk activated carbon using H3PO4 activation: a rotatable central composite design approach. Mater Chem Phys 282(February):125989. https://doi.org/10.1016/j.matchemphys.2022.125989

El-Naas MH, Alhaija MA, Al-Zuhair S (2017) Evaluation of an activated carbon packed bed for the adsorption of phenols from petroleum refinery wastewater. Environ Sci Pollut Res 24(8):7511–7520. https://doi.org/10.1007/s11356-017-8469-8

Gaikwad MS, Balomajumder C (2017) Simultaneous electrosorptive removal of chromium(VI) and fluoride ions by capacitive deionization (CDI): multicomponent isotherm modeling and kinetic study. Sep Purif Technol 186:272–281. https://doi.org/10.1016/j.seppur.2017.06.017

Gama BMV, Sales DCS, Nascimento GE, Rodriguez-Díaz JM, Barbosa CMBM, Marta MMB (2022) Modeling mono- and multicomponent adsorption of phenol and cadmium from aqueous solution by peanut shell biochar. Ind Eng Chem Res 61(51):18833–18842. https://doi.org/10.1021/acs.iecr.2c02618

Gupta A, Balomajumder C (2015) Simultaneous adsorption of Cr(VI) and phenol onto tea waste biomass from binary mixture: multicomponent adsorption, thermodynamic and kinetic study. J Environ Chem Eng 3(2):785–796. https://doi.org/10.1016/j.jece.2015.03.003

Haro NK, Dávila IVJ, Nunes KGP, Espina MA, de Franco N, Marcilio R, Féris LA (2021) Kinetic, equilibrium and thermodynamic studies of the adsorption of paracetamol in activated carbon in batch model and fixed-bed column. Appl Water Sci 11(2):1–9. https://doi.org/10.1007/s13201-020-01346-5

Kakavandi B, Jafari AJ, Kalantary RR, Nasseri S, Esrafili A, Gholizadeh A, Azari A (2016) Simultaneous adsorption of lead and aniline onto magnetically recoverable carbon: optimization, modeling and mechanism. J Chem Technol Biotechnol 91(12):3000–3010. https://doi.org/10.1002/jctb.4925

Kaszkur Z, Rzeszotarski P, Juszczyk W (2014) Powder diffraction in studies of nanocrystal surfaces: chemisorption on Pt. J Appl Crystallogr 47(6):2069–2077. https://doi.org/10.1107/S1600576714023917

Khan AR, Al-Bahri TA, Al-Haddad A (1997) Adsorption of phenol based organic pollutants on activated carbon from multi-component dilute aqueous solutions. Water Res 31(8):2102–2112. https://doi.org/10.1016/S0043-1354(97)00043-2

Koli P, Bhardwaj NR (2018) Status and use of pesticides in forage crops in India. J Pestic Sci 43(4):225–232. https://doi.org/10.1584/jpestics.D18-004

Körbahti BK, Aktaş N, Tanyolaç A (2007) Optimization of electrochemical treatment of industrial paint wastewater with response surface methodology. J Hazard Mater 148(1–2):83–90. https://doi.org/10.1016/j.jhazmat.2007.02.005

Kumar KV, Gadipelli S, Wood B, Ramisetty KA, Stewart AA, Howard CA, Brett DJL, Rodriguez-Reinoso F (2019) Characterization of the adsorption site energies and heterogeneous surfaces of porous materials. J Mater Chem A 7(17):10104–10137. https://doi.org/10.1039/c9ta00287a

Leong K-Y, See S, Lim J-W, Bashir MJK, Ng C-A, Tham L (2017) Effect of process variables interaction on simultaneous adsorption of phenol and 4-chlorophenol: statistical modeling and optimization using RSM. Appl Water Sci 7(4):2009–2020. https://doi.org/10.1007/s13201-016-0381-8

Li K, Zhou M, Liang L, Jiang L, Wang W (2019a) Ultrahigh-surface-area activated carbon aerogels derived from glucose for high-performance organic pollutants adsorption. J Colloid Interface Sci 546:333–343

Li Z, Sellaoui L, Dotto GL, Bonilla-Petriciolet A, Lamine AB (2019b) Understanding the adsorption mechanism of phenol and 2-nitrophenol on a biopolymer-based biochar in single and binary systems via advanced modeling analysis. Chem Eng J 371(March):1–6

Li M, Wang Y, Liu Y, Wang H, Song H (2022a) Preparation of active carbon through one-step NaOH activation of coconut shell biomass for phenolic wastewater treatment. Res Chem Intermed 48(4):1665–1684. https://doi.org/10.1007/s11164-021-04650-0

Li Z, Mao Y, Yan X, Song Z, Liu C, Liu Z, Kang H et al (2022b) Design a flower-like magnetic graphite carbon microsphere for enhanced adsorption of 2,4-dichlorophenol. Environ Sci Pollut Res 29(55):83138–83154. https://doi.org/10.1007/s11356-022-21364-x

Li Z, Yanli M, Zuwen L, Zhongxian S (2024) Efficient adsorption and removal mechanism of 2,4-dichlorophenol by MoS2@C6H12O6 floral activated carbon with intercalated structure. Mater Sci Eng B 299:116807. https://doi.org/10.1016/j.mseb.2023.116807

Liadi MA (2020) Comparative performance study of ZnCl2 and NaOH sludge based activated carbon for simultaneous aqueous uptake of phenolic compounds. Int J Environ Anal Chem 00(00):1–25. https://doi.org/10.1080/03067319.2019.1704746

Liu C, You J, Ruirui Hu, Jiang W, Duan Y, Li J, Li Z et al (2021) Removal of bisphenol a and 2, 4-dichlorophenol from lake water using a flower-like covalent organic framework. Anal Lett 54(3):347–363. https://doi.org/10.1080/00032719.2020.1764969

Luo Y, Li D, Chen Y, Sun X, Cao Q, Liu X (2019) The performance of phosphoric acid in the preparation of activated carbon-containing phosphorus species from rice husk residue. J Mater Sci 54(6):5008–5021. https://doi.org/10.1007/s10853-018-03220-x

Mandal A, Majumder A, Banik I, Ghosh K, Bar N, Das SK (2021) Fixed-bed column study for removal of phenol by neem leaves–experiment, MLR and ANN analysis. Sustain Chem Pharm 23(August):100514. https://doi.org/10.1016/j.scp.2021.100514

Mandal A, Nirjhar B, Sudip KD (2020) Phenol removal from wastewater using low-cost natural bioadsorbent neem (azadirachta indica) leaves: adsorption study and MLR modeling. Sustain Chem Pharm 17:214. https://doi.org/10.1016/j.scp.2020.100308

Melo JM, Lütke SF, Igansi AV, Franco DSP, Vicenti JRM (2024) Mass transfer and equilibrium modelings of phenol adsorption on activated carbon from olive stone. Colloids Surf A Physicochem Eng Aspects 680:132628. https://doi.org/10.1016/j.colsurfa.2023.132628

Meng ZF, Zhang YP, Zhang ZQ (2008) Simultaneous adsorption of phenol and cadmium on amphoteric modified soil. J Hazard Mater 159(2–3):492–498. https://doi.org/10.1016/j.jhazmat.2008.02.045

Mishra L, Paul KK, Jena S (2022) Adsorption isotherm, kinetics and optimization study by box behnken design on removal of phenol from coke wastewater using banana peel (*Musa* Sp.) biosorbent. Theor Found Chem Eng 56(6):1189–1203. https://doi.org/10.1134/S0040579522330041

Mourão P, Cassavela C, Cansado I, Castanheiro J, Ribeiro L, Pagnanelli F (2024) Adsorption of bisphenol A by granular activated carbon prepared with different silicates as binders. Int J Environ Sci Technol 21(4):3719–3734. https://doi.org/10.1007/s13762-023-05212-0

Namasivayam C, Kavitha D (2006) IR, XRD and SEM studies on the mechanism of adsorption of dyes and phenols by coir pith carbon from aqueous phase. Microchem J 82(1):43–48. https://doi.org/10.1016/j.microc.2005.07.002

Nguyen ML, Huang C, Juang RS (2016) Synergistic biosorption between phenol and nickel(II) from binary mixtures on chemically and biologically modified chitosan beads. Chem Eng J 286:68–75. https://doi.org/10.1016/j.cej.2015.10.065

Nirmala G, Thanapalan Murugesan K, Rambabu KS, Show PL (2021) Adsorptive removal of phenol using banyan root activated carbon. Chem Eng Commun 208(6):831–842. https://doi.org/10.1080/00986445.2019.1674839

Ortiz-Martínez K, Reddy P, Cabrera-Lafaurie WA, Román FR, Hernández-Maldonado AJ (2016) Single and multi-component adsorptive removal of bisphenol A and 2,4-dichlorophenol from aqueous solutions with transition metal modified inorganic-organic pillared clay composites: effect of PH and presence of humic acid. J Hazard Mater 312(July):262–271. https://doi.org/10.1016/j.jhazmat.2016.03.073

Patil P, Jeppu GP, Ramachandra Murthy V, Girish CR (2023) A review on interaction of phenolic pollutant with other pollutants in the binary adsorption system. Desalin Water Treat 285:213–241. https://doi.org/10.5004/dwt.2023.29313

Patil P, Jeppu G, Vallabha MS, Girish CR (2024) Enhanced adsorption of phenolic compounds using biomass-derived high surface area activated carbon: isotherms, kinetics and thermodynamics. Environ Sci Pollut Res 31(60):67442–67460. https://doi.org/10.1007/s11356-024-32971-1

Pei T, Feng S, Defa H, Fulin Y, Yi L, Can L, Xu L, Yanling L, Zhifeng Z, Yunwu Z (2023) Enhanced adsorption of phenol from aqueous solution by KOH combined Fe-Zn bimetallic oxide co-pyrolysis biochar: fabrication, performance, and mechanism. Bioresource Technol 388:63. https://doi.org/10.1016/j.biortech.2023.129746

Rawi MF, Ghayda YAK, Jwad KAR, Tariq AH, Husam AAH (2023) Adsorption, isotherms, and kinetics for phenol removal on biochar prepared from wheat Husk. IOP Conf Ser Earth Environ Sci. https://doi.org/10.1088/1755-1315/1222/1/012012

Shaarani FW, Hameed BH (2010) Batch adsorption of 2,4-dichlorophenol onto activated carbon derived from agricultural waste. Desalination 255(1–3):159–164. https://doi.org/10.1016/j.desal.2009.12.029

Shahbazi A, Niloufar NM, Zeinab S (2019) Synergistic and antagonistic effects in simultaneous adsorption of Pb(II) and Cd(II) from aqueous solutions onto chitosan functionalized EDTA-silane/MGO. Biocatal Agric Biotechnol 22:101398. https://doi.org/10.1016/j.bcab.2019.101398

Singanodi M, Pratheek V, Nagaraj C, Kumar A, Mallikarjunappa K (2023) Competitive and cooperative adsorption analysis for dye removal from multicomponent system using prosopis Juliflora activated carbon. Environ Sci Pollut Res 30(39):90362–90382. https://doi.org/10.1007/s11356-022-24721-y

Singh N, Balomajumder C (2016) Simultaneous biosorption and bioaccumulation of phenol and cyanide using coconut shell activated carbon immobilized pseudomonas putida (MTCC 1194). J Environ Chem Eng 4(2):1604–1614. https://doi.org/10.1016/j.jece.2016.02.011

Sriramoju SK, Dash PS, Majumdar S (2021) Meso-porous activated carbon from lignite waste and its application in methylene blue adsorption and coke plant effluent treatment. J Environ Chem Eng 9(1):104784. https://doi.org/10.1016/j.jece.2020.104784

Sukpreabprom H (2015) Single and binary adsorption of Cd (II) and Zn (II) ions from aqueous solutions onto bottom ash. Korean J Chem Eng 32(5):896–902. https://doi.org/10.1007/s11814-014-0309-7

Suresh S, Srivastava VC, Mishra IM, Pratap-Singh A (2021) Multicomponent column optimization of ternary adsorption based removal of phenolic compounds using modified activated carbon. J Environ Chem Eng 9(1):104843. https://doi.org/10.1016/j.jece.2020.104843

Tao J, Huo P, Zongheng Fu, Zhang J, Yang Z, Zhang D (2019) Characterization and phenol adsorption performance of activated carbon prepared from tea residue by NaOH activation. Environ Technol 40(2):171–181. https://doi.org/10.1080/09593330.2017.1384069

Tichapondwa SM, Siyabulela T, Washington M (2018) Adsorption of phenol and chromium (VI) pollutants in wastewater using exfoliated graphite. Chem Eng Trans 70:847–52. https://doi.org/10.3303/CET1870142

Vohra M, Hussaini M, Mohammad T (2023) Olive branches activated carbon: synthesis, phenol adsorption and modeling. Chem Pap 77(1):485–498. https://doi.org/10.1007/s11696-022-02457-w

Wu C, Luman Z, Chen Z, Yun Z, Siqing X, Bruce ER (2022) Co-removal of 2,4-dichlorophenol and nitrate using a palladized biofilm: denitrification-promoted microbial mineralization following catalytic dechlorination. J Hazard Mater 422:126916. https://doi.org/10.1016/j.jhazmat.2021.126916

Xie J, Chao L, Wenqian C, Binbin H (2022) Conductive-polymer-supported palladium-iron bimetallic nanocatalyst for simultaneous 4-chlorophenol and Cr(VI) removal: enhanced interfacial electron transfer and mechanism. J Hazard Mater 424:127748. https://doi.org/10.1016/j.jhazmat.2021.127748

Xin DF, Yan L, Zhou XH, Huang ST, Liang JY, Zhang WX, Guo ZW et al (2021) Simultaneous adsorption of Cr(VI) and phenol by biochar-based iron oxide composites in water: performance, kinetics and mechanism. J Hazard Mater 416(January):125930. https://doi.org/10.1016/j.jhazmat.2021.125930

Xiong Y-K, Ping Du, Huang S-J, He S-F, Li X, Yang J, Yang Ye (2024) Polyhydroxy-azo porous organic polymers for efficient removal of organic pollutants from water. ACS Appl Polym Mater 6(10):5674–5683. https://doi.org/10.1021/acsapm.4c00329

Yadav A, Bagotia N, Sharma AK, Kumar S (2021) Simultaneous adsorptive removal of conventional and emerging contaminants

in multi-component systems for wastewater remediation: a critical review. Sci Total Environ 799:149500. https://doi.org/10.1016/j.scitotenv.2021.149500

Zhang Y, Fan J, Minglai Fu, Ok YS, Hou Y, Cai C (2019) Adsorption antagonism and synergy of arsenate(V) and cadmium(II) onto fe-modified rice straw biochars. Environ Geochem Health 41(4):1755–1766. https://doi.org/10.1007/s10653-017-9984-8

Zhang K, Qian W, Yaqian Z, Jiajun G, Chunxi L, Xingmao J (2020) A low-cost crosslinked polystyrene derived from environmental wastes for adsorption of phenolic compounds from aqueous solution. J Mol Liq 52:314. https://doi.org/10.1016/j.molliq.2020.113641

Zhang G, Lu Z, Tianying C, Xueyan F, Yi F, Honghao Z (2024) Effect of pyrolytic temperatures on the 2,4-dichlorophenol adsorption performance of biochar derived from populus Nigra. Environ Sci Pollut Res. https://doi.org/10.1007/s11356-024-31990-2

Zheng W, Zhang S, Deng J (2024) Analysis of the adsorption mechanism of phosphoric acid-modified bamboo charcoal for chlorogenic acid based on density functional theory. Chem Biol Technol Agric 11(1):1–13. https://doi.org/10.1186/s40538-024-00538-4

Zhou K, Zhang J, Xiao Y, Zhao Z, Mingming Zhang Lu, Wang XZ, Zhou C (2020) High-efficiency adsorption of and competition between phenol and hydroquinone in aqueous solution on highly cationic amino-poly(vinylamine)-functionalized GO-(o-MWCNTs) magnetic nanohybrids. Chem Eng J 389(January):124223. https://doi.org/10.1016/j.cej.2020.124223

Publisher's Note Springer Nature remains neutral with regard to jurisdictional claims in published maps and institutional affiliations.

Authors and Affiliations

Praveengouda Patil[1] · Gautham Jeppu[1] · Swathi Nayak[1] · Chikmagalur Raju Girish[1]

✉ Chikmagalur Raju Girish
cr.girish@manipal.edu

[1] Department of Chemical Engineering, Manipal Institute of Technology, Manipal Academy of Higher Education, Manipal, India